Hydrology Research

Hydrology Research Vol 54 No 6, 782 doi: 10.2166/nh.2023.011

Fluorescent quinine-based tracking techniques for measurement of open-channel surface flow velocities under low luminosity conditions using a UAS

Soheil Zehsaz [a,b,*], João L. M. P. de Lima [a,b], Jorge M. G. P. Isidoro [a,c], M. Isabel P. de Lima [a,b] and Ricardo Martins [d]

[a] MARE-Marine and Environmental Sciences Centre/ARNET-Aquatic Research Network, Pole MARE -UCoimbra, Polo II University of Coimbra, Rua Sílvio Lima, 3030-790 Coimbra, Portugal
[b] Department of Civil Engineering, Faculty of Sciences and Technology, University of Coimbra, Rua Luís Reis Santos, Pólo II – Universidade de Coimbra, 3030-788 Coimbra, Portugal
[c] Department of Civil Engineering, Institute of Engineering, University of Algarve, 8005-139 Faro, Portugal
[d] RISCO–Research Centre for Risks and Sustainability in Construction, Department of Civil Engineering, University of Aveiro, 3810-193 Aveiro, Portugal
*Corresponding author. E-mail: s.zehsaz@dec.uc.pt

SZ, 0000-0003-3287-7707; JLMPL, 0000-0002-0135-2249; JMGPI, 0000-0002-6901-5652; MIPd, 0000-0002-5134-4175; RM, 0000-0002-2871-668X

ABSTRACT

This study presents techniques based on the use of fluorescent quinine as a visual tracer for surface flows, to assess surface flow velocities in channels and streams under low luminosity conditions. Fieldwork was conducted in three open channels, with different hydraulic characteristics. A quinine solution, in both liquid and solid (ice cube) forms, was applied on the water flow surface and an Unmanned Aerial System (UAS) was used to record the movement of the fluorescent quinine. The results were compared to the velocities estimated using the thermal tracer technique and flowmeter-based velocity maps. The findings show that the quinine solution, in both liquid and solid forms, can be used to estimate open-channel surface flow velocities under low luminosity conditions. While the solid form of the quinine tracer was applied in a smaller volume than the liquid tracer, its fluorescence effect persisted longer. By comparison, the liquid tracer had the advantage of continual availability and was devoid of the constraint of melting.

Key words: leading-edge velocities, night-time monitoring, open-channel flow, quinine, remote sensing, tracers

HIGHLIGHTS

- Using a UAS for surface flow velocity measurements can improve data recording in hard-to-reach survey sites.
- The new quinine-based tracer allows us to observe the spatiotemporal water movement in open channels and to estimate surface flow velocities under low luminosity conditions.
- Quinine tracer has high visibility under UVA light in low luminosity conditions.

GRAPHICAL ABSTRACT

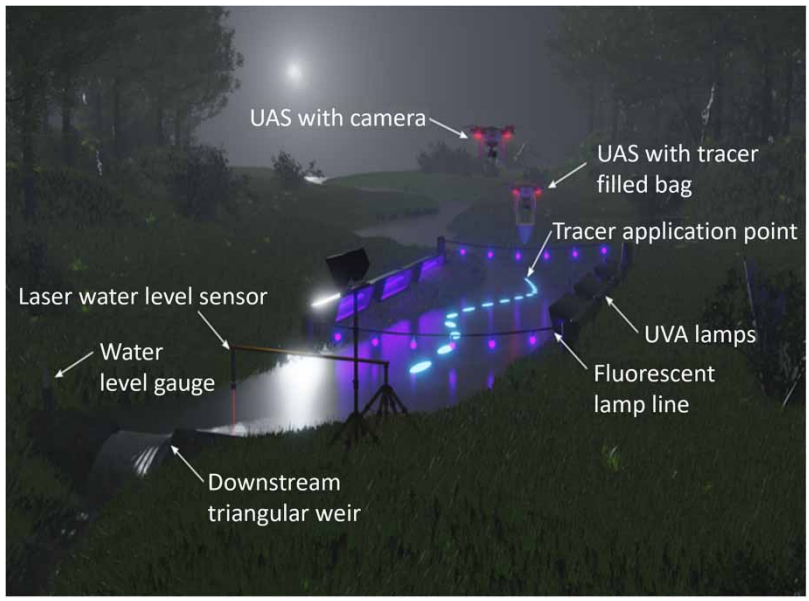

INTRODUCTION

Accurate measurement of surface water flow velocities and discharges is essential for both engineering purposes and environmental monitoring. Precise estimations of flow velocities are particularly important for understanding and modelling runoff.

Tracers are commonly used in hydrological studies to estimate surface flow velocities. Various types of tracers are used, including non-fluorescent tracers such as dye (e.g., de Lima & Abrantes 2014; Abrantes *et al.* 2018), fluorescent dye tracers (e.g., Leibundgut *et al.* 2009; Zhang *et al.* 2010), buoyant particles (e.g., Tauro *et al.* 2012; Mujtaba & de Lima 2018), salt tracers and electrolytes (e.g., Lei *et al.* 2010; Schuetz *et al.* 2012; Abrantes *et al.* 2018), and thermal tracers (e.g., Schuetz *et al.* 2012; de Lima & Abrantes 2014; de Lima *et al.* 2015; Abrantes *et al.* 2018; Mujtaba & de Lima 2018; Abrantes *et al.* 2019).

Fluorescent dye tracers are common in hydrology for identifying connections between groundwater supply points (e.g., sinkholes and karst windows), discharge points (e.g., springs and wells), and estimating sheet flow velocities (e.g., Gilley *et al.* 1990; Buzády *et al.* 2006; Leibundgut *et al.* 2009; Zhang *et al.* 2010; de Lima *et al.* 2021; Zehsaz *et al.* 2022). Several environmental non-hazardous dyes such as uranine, rhodamine WT, eosin, CI Direct Yellow 96, as well as other optical brighteners, are widely accessible and used. The environmental impact of fluorescent tracers is considered tolerable since the quantity of fluorescent material used in hydrological studies is insignificant (e.g., Aley & Fletcher 1976; Buzády *et al.* 2006; Leibundgut *et al.* 2009).

In recent decades, remote sensing techniques using Unmanned Aerial Systems (UASs) have emerged as a valid and cost-effective alternative to *in situ* environmental measurements, including river discharge, streamflow velocities (e.g., Tauro *et al.* 2015; Fulton *et al.* 2020; Masafu *et al.* 2022), and water quality parameters (e.g., Su 2017). Some studies provide an overview of the contribution of UASs regarding natural and agricultural ecosystems monitoring (e.g., Manfreda *et al.* 2018; Tmušić *et al.* 2020). UAS, equipped with a gimbal-mounted camera, are now relatively inexpensive and able to record high-resolution images and videos.

de Lima *et al.* (2021) recently presented a proof of concept for using quinine solution as a fluorescent tracer for shallow overland flows over bare soil conditions, while Zehsaz *et al.* (2022) explored its potential for estimating sheet flow velocities over mulched, vegetated, and paved surfaces. The results from this technique were found to be positively correlated with the results of the dye and thermal tracer techniques in both studies. The results indicate that using quinine solution as a fluorescent tracer offers several advantages, such as high visibility under ultraviolet A (UVA) light and under low luminosity conditions, low cost, and neglectable environmental impact. However, the quinine tracer requires UVA artificial illumination during the experimental procedure, creating an inherent limitation to the fluorescent tracer technique.

This experimental study builds on the work of de Lima *et al.* (2021) and Zehsaz *et al.* (2022) by further exploring the capability of quinine-based tracers. Both liquid and solid forms of quinine solution were used as fluorescent tracers to estimate surface velocities in flowing surface water bodies, such as rivers, irrigation channels, and drainage channels. This study explores several application methods to test the tracer's effectiveness in estimating open-channel flow surface velocities under low luminosity field conditions using a UAS. This study's primary objectives are: (i) to evaluate the tracer's ability to estimate flow surface velocities in low luminosity conditions, (ii) to investigate different tracer application methods, and (iii) to compare results obtained using two quinine-based tracers: liquid and solid (ice cubes).

MATERIALS AND METHODS

Location of field study sites and experimental setup

A conceptual illustration of the field setups required to conduct fluorescent tracer-based experiments for estimating surface flow velocities in open channels is shown in Figure 1. Different quinine-based tracers (e.g., liquid and solid) and tracer application methods (e.g., point and linear) were compared. The experiments were conducted at three locations: (i) an irrigation concrete-lined channel (40°13′01.4″N, 8°26′23.2″W), with a surface water width of 7 m; (ii) a drainage earth channel – site 1 (40°13′09.7″N, 8°27′14.4″W), with a surface water width of 3.5 m; and (iii) a drainage earth channel – site 2 (40°13′03.1″N, 8°26′38.6″W) with a surface water width of 3.9 m. The locations and views of all three study sites are shown in Figures 2 and 3. The selection of the three sites was based on several criteria, including (1) easy access to the measuring site for installing the experimental setup and applying the tracers; (2) less vegetation cover on the margins of the channels (to avoid hindering a clear view of the flow from the UAS); (3) a small number of obstacles around the selected location (such as buildings or trees,

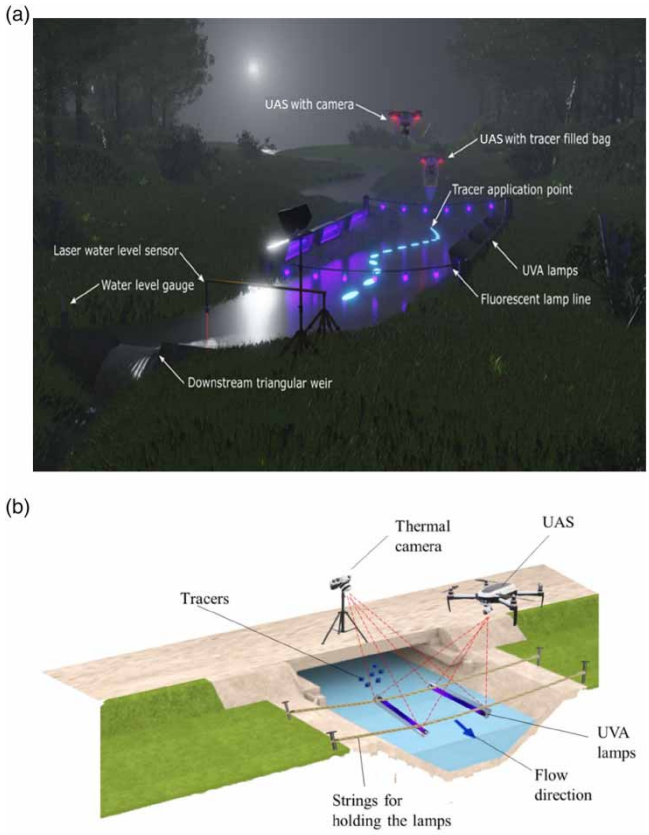

Figure 1 | (a) Pictorial conceptual representation of the types of field setups needed for conducting fluorescent (quinine) tracer field observations, (b) illustration of the field setups used in this study: UAS was used in the drainage channel and the thermal (infrared) camera was used in the irrigation channel.

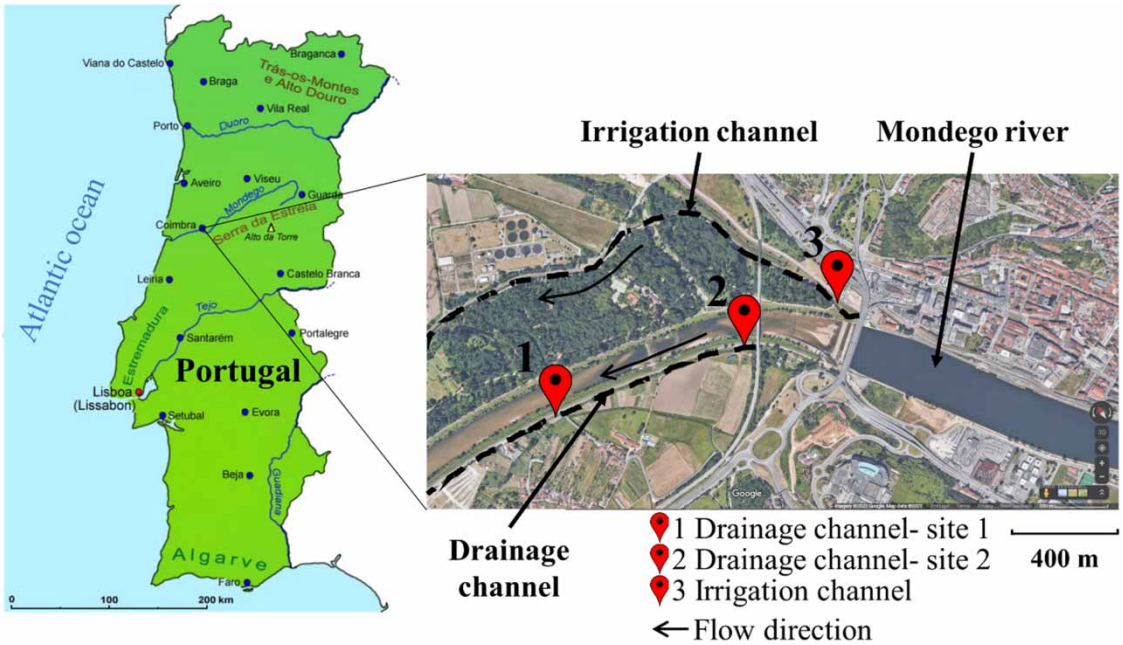

Figure 2 | Location of the three selected study sites (Coimbra, Portugal).

Figure 3 | Views of the three selected sites in open channels: (a) drainage channel – site 1; (b) drainage channel – site 2; (c) irrigation channel. Drainage channel sites 1 and 2 are, respectively, downstream and upstream sections of the same drainage ditch.

to reduce the risk of crashing the UAS during the flights); and (4) different open-channel hydraulic conditions (velocity, flow) in each study site (Table 1).

To expose the fluorescent tracer, two UVA lamps with a Blacklight Blue (BLB) light bulb were used, with one lamp on each side of the measuring frame, aligned parallel to the flow direction (see Figure 1(b)). These lamps are characterised by a nominal power of 36 W, UVA irradiance at 20 cm, 315–400 nm: 350 mW/cm^2; and peak emission wavelength of 0.354 μm. The two lamps, pointing to the water surface, were installed close to the centre of the channels, separated by 1.2 m (each lamp 0.6 m from the centre of the channel), and suspended from high-resistance strings attached to metal bars on channel margins. A measuring frame (i.e., observation area) with 1.0 m × 1.0 m was located between the lamps. A UAS was used to monitor (video record) the tracer application in the selected locations of the channels.

Table 1 | Hydraulic conditions of the three selected sites in open channels

Location	Channel structure	Channel shape	Discharge (m^3/s)	Water surface width (m)	Max water depth (m)	Temperature (°C)	
						Water	Ambient
Irrigation channel	Concrete	Trapezoidal	4.25	7.0	2.0	19	14
Drainage channel – site 1	Earth channel (soil)	U-shape	0.59	3.9	0.7	20	19
Drainage channel – site 2	Earth channel (soil) with a rocky bed	U-shape	0.52	3.5	0.5	20	19

Tracers

Quinine is extracted from cinchona tree and is used in medicine for treatment purposes (e.g., Diener *et al.* 2002; Geto *et al.* 2012) and as a bitter flavouring agent in soft drinks such as tonic water (EFSA 2015). The fluorescence property of a diluted solution of quinine allows the tracking of the tracer on the surface of flowing water. Quinine-based tracers, in liquid and solid (ice cubes) forms, used monohydrochloride dihydrate 99% (ACROS Organics™). This form of quinine, used in small quantities and low concentrations, has no ecotoxicological effects on the environment and is not likely to be mobilised in the soil due to its low water solubility (Thermo Fisher Scientific 2021). Quinine luminosity was optimised by setting the solution pH at 3.7 and the concentration at 80 mg/L. It was observed, similarly to Moorthy *et al.* (1998), that even a small difference in the pH makes a substantial difference in its luminescence. Therefore, to ensure that the properties that maximise the luminescence were kept as long as possible during the measurements, the quinine solution was frozen. The size of the ice cubes used in all the experiments was $0.04\ m \times 0.035\ m \times 0.01\ m$ ($\approx$14 mL) (for simplicity the informal expression 'ice cubes' is here used, notwithstanding that iced regular hexahedrons were not used). The ice cubes showed a similar fluorescence effect to the liquid form of the solution (Figure 4) and could be used as a thermal tracer (e.g., Abrantes *et al.* 2019). Results obtained by the two techniques, based on the fluorescence and thermal attributes of the quinine tracer, were compared.

Tracer application methods

The quinine-based tracers were tested under similar conditions (e.g., same straight channel section; approximately the same discharge, flow depths and velocities). Several methods for applying the liquid and solid quinine tracers into the flow surface were tested during the field experiments (Table 2), namely, point and linear applications. The liquid tracer volumes used with the point and linear application methods were 250 and 450 mL, respectively. The quantity of the liquid tracer solution used was the minimum that allowed tracking the tracer during the experiments. In the solid tracer release door container method, the ice cubes were released from approximately 0.20 m above the water surface. In the solid spill container, the ice cubes were spilt on the water surface at one point. For all cases, the application of the tracers was conducted carefully to minimally disrupt the flow.

Flow measurement

An electromagnetic flowmeter (Valeport Model 801) was used to measure flow velocities in the studied drainage open channels, in the selected cross-sections (sites 1 and 2) and draw the surface velocity fields. Due to access difficulties, the flowmeter

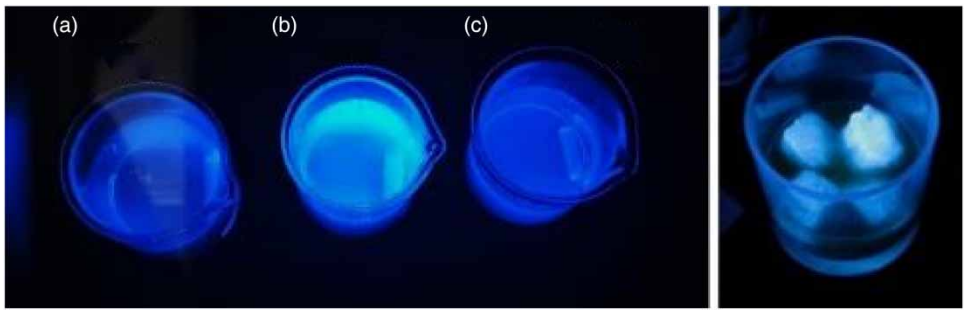

Figure 4 | Visualisation of the quinine tracer in different forms and glow intensities with different pH values and the same quinine concentration (80 mg/L). Left image: quinine liquid solutions of (a) pH = 2.3; (b) pH = 3.7; (c) pH = 4.7; right image: ice cubes made of quinine solution with a pH of 3.7. All tracers are under UVA light.

Table 2 | Tracer forms (liquid and solid) and methods of tracer application (point and linear) into the flowing water surface used during the field experiments

Tracer form	Tracer application method	
	Point	Linear
Liquid	 Spill container	 Liquid spill container series  Box container  Moving can
Solid	 Spill container  Release door container	 Solid spill container series

was not used in the irrigation channel. The technical specifications of the flowmeter are as follows: measuring range of −5 to +5 m/s; accuracy of ±0.5%; sensing volume: cylinder of approximately 20 mm diameter × 10 mm height and minimum measuring water depth of 5 cm.

UAS and video recording systems

The real imaging video and photographs were recorded using a camera with a gimbal installed on a DJI Phantom 4 Pro quadcopter UAS controlled manually with the DJI GO 4 mobile application. The equipment specifications are presented in Table 3.

The thermal videos were recorded with the FLIR DUO PRO R infrared camera (resolution: 336 × 256 pixels; accuracy: ±5 °C or 5% of readings in the −25 to +135 °C range; spectral range: 7.5–13.5 μm). The cameras were installed with the sensor parallel to the water surface.

To gather the data needed for this study, the UAS was used to record real videos of quinine tracer movement in the drainage channel and the FLIR DUO R infrared camera was installed on a bridge over the irrigation channel to capture thermal and real video images simultaneously.

Table 3 | Technical specifications of the Phantom 4 Pro UAS and camera systems

Aircraft		Gimbal		Camera	
Weight (battery and propellers included)	1,375 g	Stabilisation	Three-axis	Sensor	1-inch CMOS Effective pixels: 20M
Diagonal size (propellers excluded)	350 mm	Controllable range	−90° to +30°	Lens	FOV 84° 8.8 mm/24 mm (35 mm format equivalent) f/2.8
Max. speed	S-mode: 20 m/s A-mode: 16 m/s P-mode: 14 m/s	Max. controllable angular speed	90°/s	Image size	3:2 Aspect Ratio: 5,472 × 3,648 pixels
Max. wind speed resistance	10 m/s			Video recording mode	C4K: 4,096 × 2,160 pixels Max video bitrate: 100 Mbps
Max. flight time	Approx. 30 min				

Field experimental procedure

At the selected cross-sections of the drainage channel, the water surface width was measured, as well as the depth of the water at regular spatial intervals (every 0.40 m) between the banks. The electromagnetic flowmeter was used to measure the flow velocities at several points in the cross-section; 23 and 25 measurements were taken, respectively, for drainage channel – sites 1 and 2. Cross-section velocity maps were created based on these measurements; for the wall and bed boundary layer of the channels, the flow velocity was assumed 0 m/s. A physical interpolation method, Thin Plate Spline (TPS) algorithm, was applied to the data to create the flow velocity maps.

The discharge in the drainage channels was estimated by spatially integrating the measured flow velocities. Tracers were applied carefully on the water surface, using an extension wooden bar, 0.2 m upstream of the measuring frame to minimise any interference in the stream. The movement of the tracers along the measuring frame was recorded with the FLIR DUO R infrared camera for the irrigation channel and with the real video camera installed on the UAS for the drainage channel. During the field experiments, three replicates of video recordings were conducted for each test (form and method of tracer application). While recording the fluorescent tracers in the drainage channels, the UAS was flying in P-mode, (e.g., maintaining a fixed GPS-controlled position) above the water surface with the camera's sensor parallel and 2.6 m above the water surface. The infrared camera was fixed to a tripod on the top of a bridge over the irrigation channel, recording real and thermal videos, with the camera's lenses 4 m above, and parallel to, the water surface. The water temperature in the selected cross-sections and the ambient temperature were measured (Table 1). The infrared camera provided data on the water temperature, while a cell phone application was used to collect information on the ambient temperature. The experiments were conducted without interference from the wind on the water surface.

Velocity estimation and image processing method

The flow velocities were calculated from the video snapshots, for all quinine-based and thermal tracers. Methods of velocity estimation for all tracer forms and applications are illustrated in Figure 5.

The surface velocity V_s was estimated by calculating the travel distance of the tracers' plume leading-edge (leading vertex) or leading-front (averaged discrete points, in the linear applications) over time Δt, within the measuring frame (de Lima *et al.* 2021; Zehsaz *et al.* 2022). When using solid tracers, the travel distance of each ice cube over time Δt was calculated separately, according to the procedure described in de Lima *et al.* (2023). The surface velocity V_s was considered as the average of the velocities estimated for a group of ice cubes, in both the point and linear application methods.

Methodology overview

Figure 6 shows a schematic flowchart that illustrates the methodological steps applied in this work for (i) estimating open channels' surface flow velocities using tracers and (ii) estimating cross-section velocity profiles and discharge, using a hydraulic flow velocity meter (i.e., flowmeter). In fieldwork, to collect images of the water surface observation area, the use of a camera installed on a UAS might be considered when the conventional deployment of a camera is not viable. The flowchart describes field work, data processing and outputs.

RESULTS AND DISCUSSION

Figure 7 shows recorded images from drainage channel – site 2, for the different forms and applications of quinine tracer into the flow (see Table 2). Each pair of images (Figure 7(a)–7(g)) highlights (in red) the displacement, for a time step of $\Delta t = 1$ s, of the: tracer plume for point application of liquid tracer (a); leading-front of the tracer plume for linear application of liquid tracer (b–d); ice cubes, for point application of ice cubes (e and f), and linear application of ice cubes (g). This set of images (Figure 7) shows that both solid and liquid forms of quinine tracer can be easily detected under low luminosity conditions with a UVA light.

When tracing the leading-edge diffusion limits the time frame to perform the measurements, as well as introducing difficulties in the measurement. However, the movement of marked points on the tracer's leading front line was accurately monitored, as depicted in Figure 7(b)–7(d). Point and linear applications presented distinct difficulties with the former detection being considerably more straightforward than the latter.

Unlike the liquid form of tracers, the ice cubes kept their shape and fluorescent concentration during the experiments, facilitating the monitoring and measuring of the travel distance of the cubes over time within the measuring frame

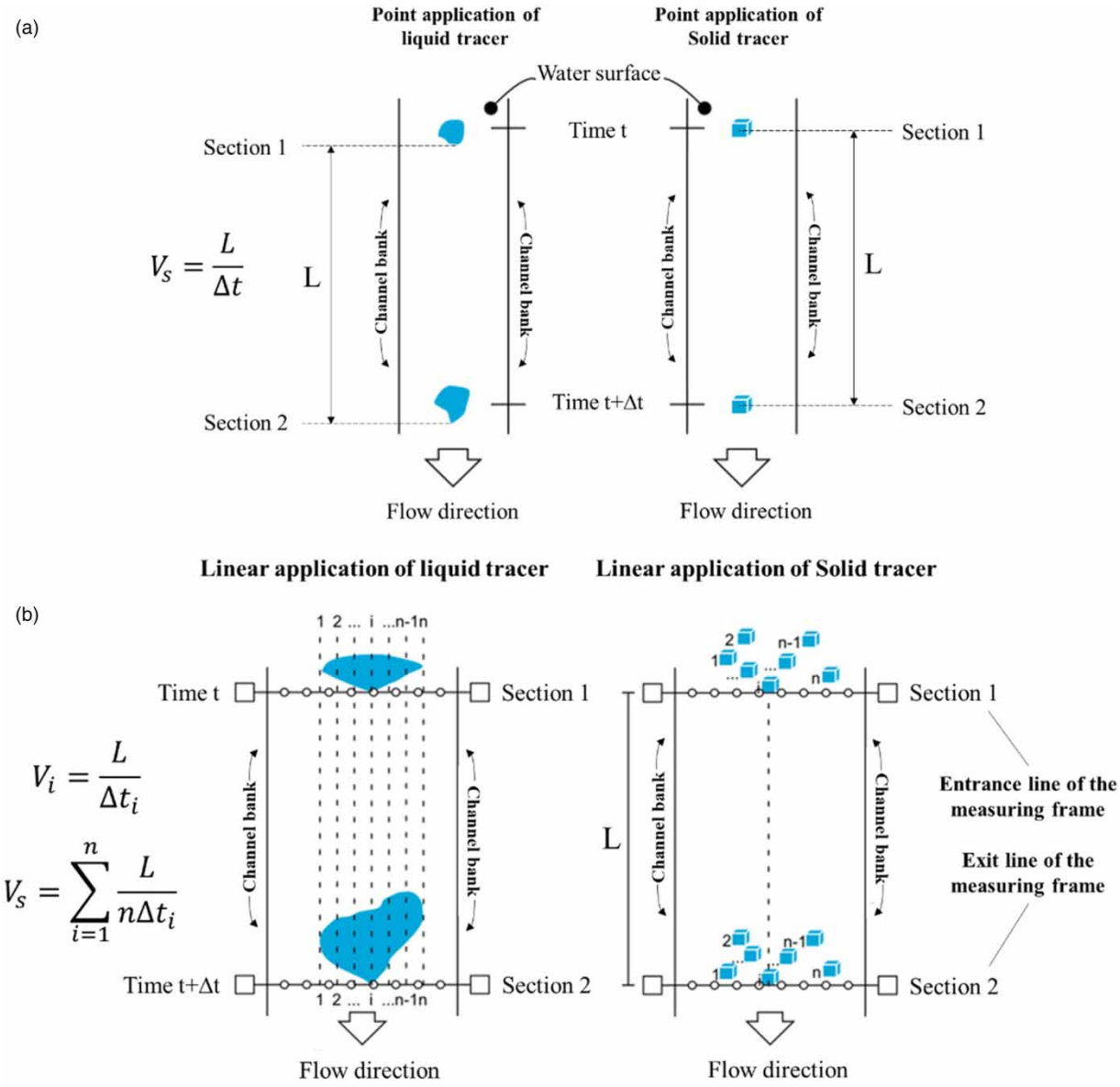

Figure 5 | Illustration of the fluorescent tracer methods for estimating surface flow velocity with liquid and solid tracers. (a) Velocity estimation of tracer point application; (b) velocity estimation of tracer linear application. In the figure, L is the travel distance of the solid tracers or leading-edge or leading-front of the liquid tracers within time Δt.

(Figure 7(e)–7(g). The differences between the spill and release door container methods are shown in Figure 7(e) and 7(f). When using the spill container method, the ice cubes moved closer to each other, resulting in a closer estimate of surface flow velocities at the point where the tracer was applied.

The flow surface velocities (V_s) obtained by applying a quinine tracer, and the procedure described in 'Field experimental procedure' section for all three experimental sites, are summarised in Table 4, where the mean and standard deviation (S.D.) for the three experimental replicates are also presented.

The FLIR DUO R infrared camera's ability to record dual images (thermal and real video images simultaneously) facilitated the comparison of two tracer techniques under the same conditions (e.g., form of tracer, application method of tracer, and volume of tracer). Specifically, thermal imaging was exclusively employed in the irrigation channel, and the results for

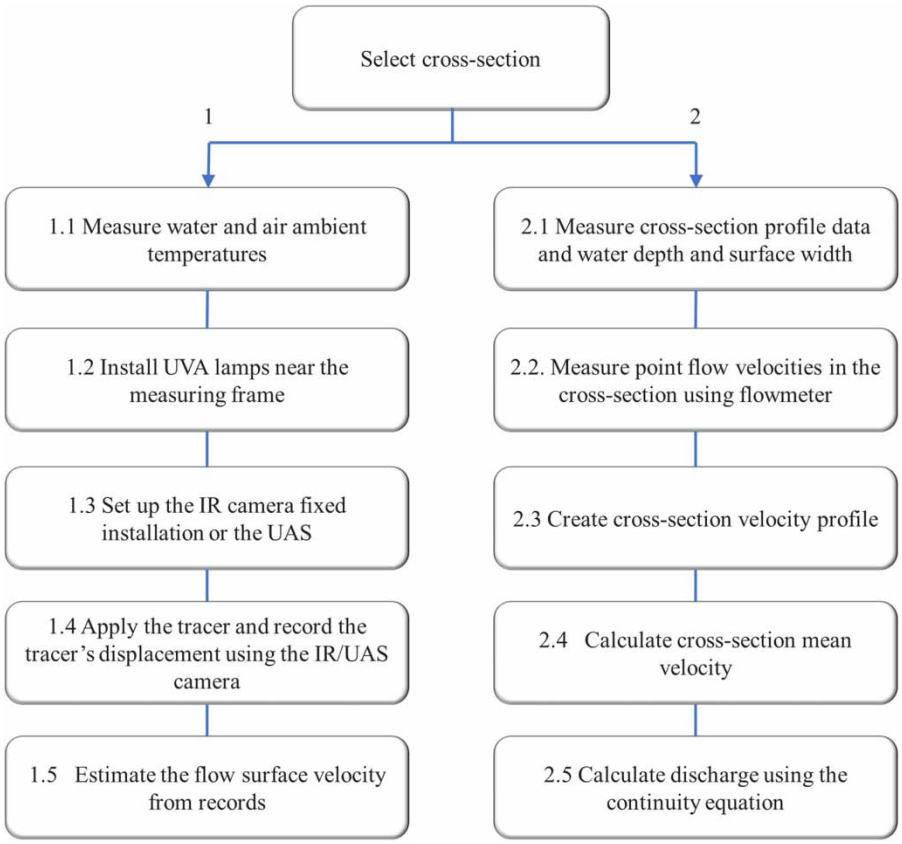

Figure 6 | Flowchart of field experimental procedure and data processing steps.

each tracer application method (point and linear) were obtained from the same set of experiments (form and volume of tracer), using both thermal and fluorescent tracing techniques.

Table 4 presents the results of the velocity estimates for the irrigation channel, obtained using the quinine and thermal tracer techniques. Figure 8 illustrates the comparison of surface velocities (V_s) estimated by applying the solid quinine and thermal tracer techniques. The obtained results showed that both applied tracing techniques (quinine and thermal) yielded highly consistent estimates, with a variation of less than 4% between them as depicted in Figure 8.

Figure 9 illustrates the flow depth and velocity distribution maps for the selected cross-sections in drainage channel – sites 1 and 2. The velocity data, measured by the electromagnetic flowmeter, enabled the comparison of the surface velocity estimations using fluorescent quinine with those obtained using the flowmeter.

The surface velocities estimated using the liquid and solid tracer forms were compared against the velocities in the positions where the tracers were applied that were extracted from the velocity distribution maps obtained from electromagnetic flowmeter measurements (Figure 10), for the drainage channel – sites 1 and 2. All tracer forms yielded similar results. This figure suggests that the liquid tracer leads to slightly higher velocity estimates in comparison to the solid tracer-based velocity estimates. This result can be interpreted as if the ice tracer is floating on the water surface and the liquid tracer moves slightly under the surface. This could be expected from the typical velocity profile in open-channel flow, due to the larger friction between the ice cube and the surface of the water with the air. Thus, the velocities estimated using ice cubes were lower than those obtained using the liquid quinine tracer.

On average, the flowmeter measurement velocities resulted between 3.5 and 8.3% higher than the estimations using the quinine tracer in drainage channel – site 1 and solid form of quinine tracer in drainage channel – site 2, respectively. However, the flowmeter yielded 2.6% lower velocities than the liquid quinine tracer in the drainage channel – site 2. This discrepancy is likely caused by experimental and instrumental measurement errors.

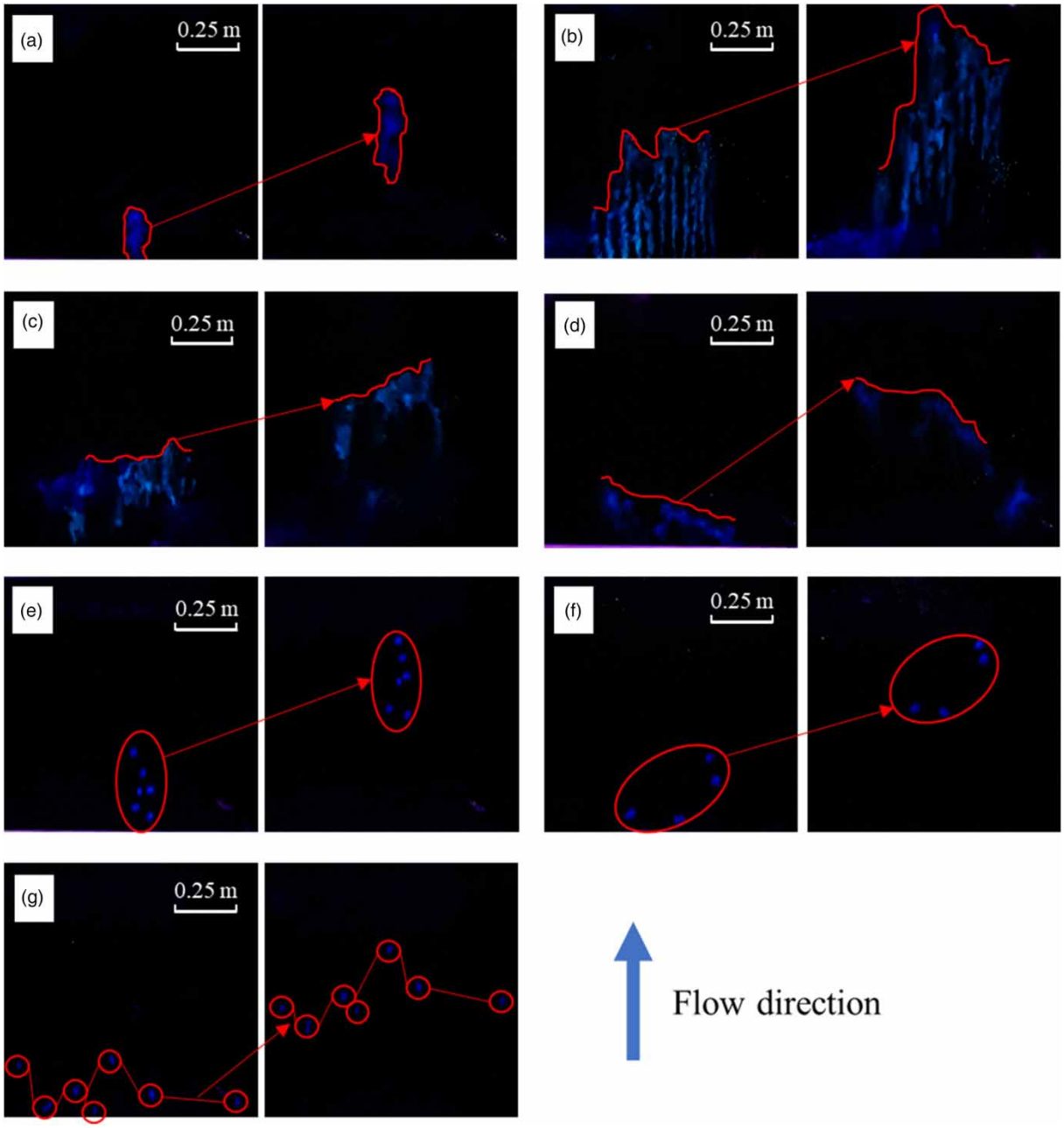

Figure 7 | Visualisation of the displacement of the tracer during a time interval $\Delta t = 1$ s (paired images), for different forms and applications of quinine solution tracer in drainage channel – site 2: (a) liquid-point, (b) liquid-linear, container series, (c) liquid-linear, box container, (d) liquid-linear, moving can, (e) solid-point, spill, (f) solid-point, release, and (g) solid-linear, container series. The horizontal and vertical scales in all images are the same. Please refer to the online version of this paper to see this figure in colour: http://dx.doi.org/10.2166/nh.2023.011.

CONCLUSIONS

In this study, a UAS was used to assess the movement of fluorescent quinine tracers in different forms and application methods and their ability to estimate open-channel surface flow velocities under low luminosity conditions. The conclusions driven by the fieldwork in different sites are:

- Quinine solution tracer exposed to UVA light can be used to estimate open-channel surface flow velocities at night or under low luminosity conditions.

Table 4 | Surface flow velocities estimated using different forms and applications of quinine tracer for the drainage earth channel – site 1 (downstream section), drainage earth channel – site 2 (upstream section) and irrigation concrete channel, and thermal tracer for the irrigation concrete channel

					Surface velocity, V_s (m/s)	
Location	**Discharge, Q (m^3/s)**	**Froude number**	**Form of tracer**	**Application method**	**Mean (three replicates)**	**S.D.**
Drainage earth channel – site 1	0.59	0.17	Solid	Point-spill	0.42	0.017
				Point-release	0.39	0.020
				Linear	0.38	0.007
				Mean (three methods)	0.40	–
				S.D.	0.012	–
			Liquid	Point	0.42	0.017
				Linear-container series	0.42	0.022
				Linear-box container	0.41	0.019
				Linear-moving can	0.39	0.007
				Mean (four methods)	0.41	–
				S.D.	0.012	–
Drainage earth channel – site 2	0.52	0.37	Solid	Point-spill	0.71	0.015
				Point-release	0.71	0.019
				Linear	0.74	0.004
				Mean (three methods)	0.72	–
				S.D.	0.012	–
			Liquid	Point	0.75	0.01
				Linear-container series	0.78	0.023
				Mean (two methods)	0.76	–
				S.D.	0.016	–
Irrigation concrete channel	4.25	0.11	Thermal	Point-spill	0.5	0.013
				Linear	0.48	0.018
				Mean (two methods)	0.49	–
				S.D.	0.01	–
			Quinine-solid	Point-spill	0.52	0.003
				Linear	0.48	0.029
				Mean (two methods)	0.5	–
				S.D.	0.02	–

Mean velocity and standard deviation (S.D.) for three replicates. The discharge was estimated by applying the area-velocity method, based on flowmeter measurements.

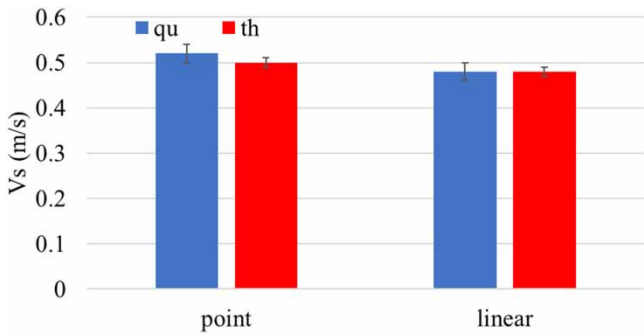

Figure 8 | Comparison of the tracer-based velocity estimates obtained from applying quinine and thermal tracers into the irrigation channel flow.

- The fluorescent-based approach for estimating surface flow velocities is a simple and low-cost technique. Essentially, all that is required are UVA lamps and a regular camera to make the observations. However, the installation of the setup, such as fixing the lamps or camera, may require considerable effort, depending on the fieldwork and local conditions. The use of a UAS can facilitate some of the setup installations, especially in cases where accessing the site is difficult. Installing cameras on a UAS does not require carrying or fixing any heavy supports, such as tripods.

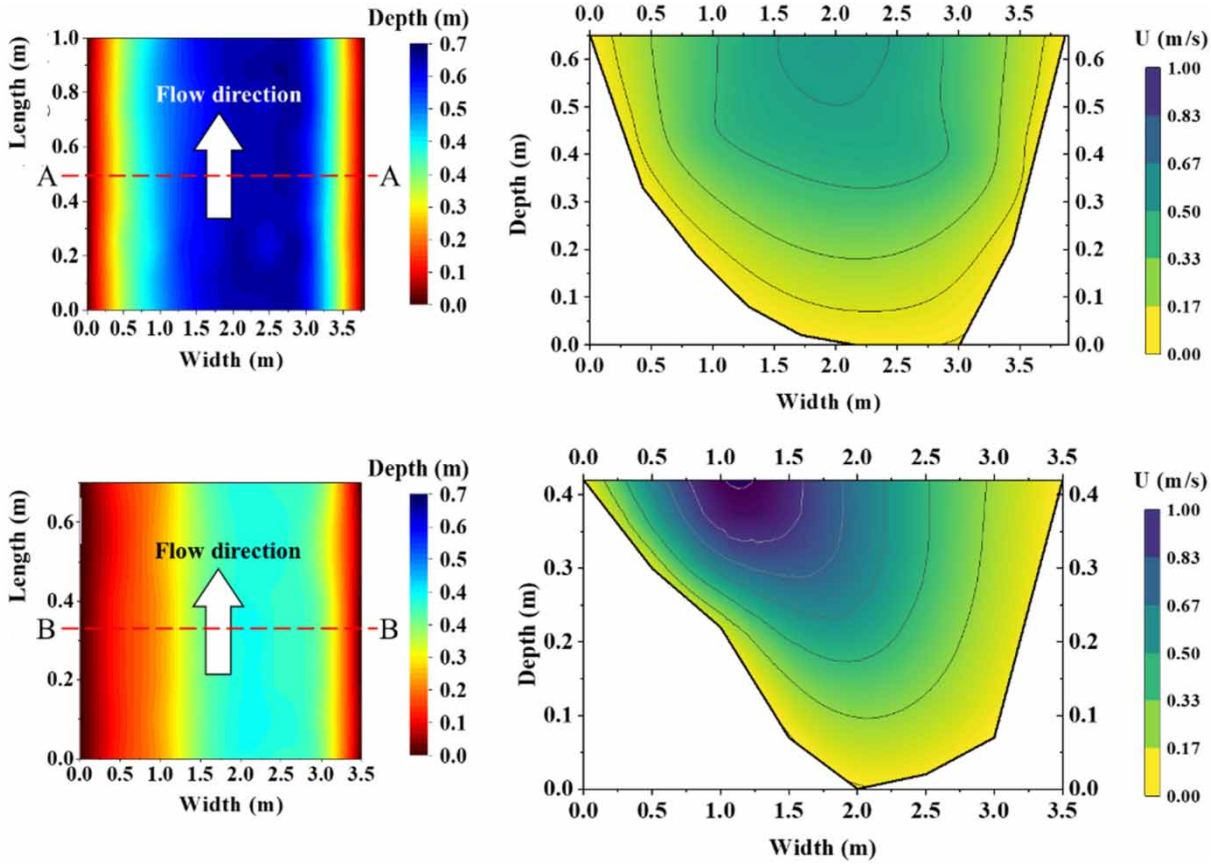

Figure 9 | Maps of flow water depths (left) and cross-section velocity profiles (right) for drainage channel – site 1, cross-section A-A (top) and site 2, cross-section B-B (bottom), estimated using a flowmeter.

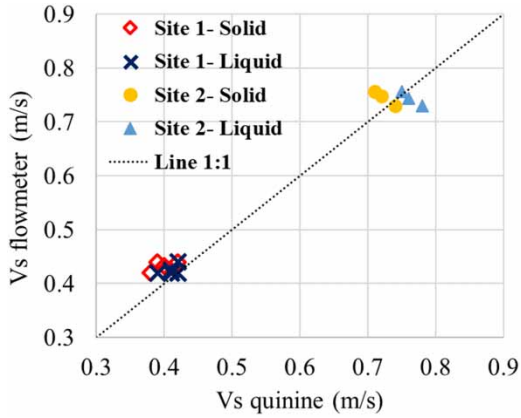

Figure 10 | Comparison between velocities measured using the quinine tracer (V_s quinine) and extracted from the velocity maps derived from the flowmeter point measurements (V_s flowmeter), for the drainage channel sites 1 and 2.

- The advantage of using the solid (ice cubes) form of the quinine tracer over the liquid form was that, although the volume of the solid tracer used in the experiment was smaller than the liquid tracer, the tracer in solid form was easier to track due to diffusion of the liquid tracer in the channel flow. The liquid tracer plume is untraceable in a few seconds after applying the tracer into the flow, whereas the ice cubes take time to melt, thus maintaining the same concentration of tracer during the measuring time (the time lapse between the instants when the leading edge of the tracer enters and exits the measuring

frame). However, in some conditions (e.g., high ambient temperatures), it might not be easy to have access to or maintain the ice cubes solid in field conditions.

- When using the liquid tracer, the leading edge of the tracer plume is difficult to distinguish after a short while of the tracer application. On the other hand, the linear application of the liquid tracer led to some difficulties when analysing the images for estimating the surface velocities because it is challenging to track the marked points on the leading front line of the tracer plume separately, within the measuring frame and time.

Based on the findings of the study and experimental conditions, the authors recommend using the solid form of the quinine solution tracer as it is easier to track and keep a constant concentration of the tracer throughout the measuring time. For measuring flow surface velocities at a specific point, the point application method is recommended, while the linear application method is suggested for obtaining surface velocities across the channel or to estimate the average velocity within the channel width.

AUTHOR CONTRIBUTIONS

S.Z., J.L.M.P.d.L., and J.M.G.P.I. conceived and designed the experiments; S.Z. performed the experiments; S.Z., J.L.M.P.d.L., and M.I.P.d.L. analysed the data; S.Z. and J.L.M.P.d.L. wrote the draft paper; J.L.M.P.d.L., J.M.G.P.I., M.I.P.d.L., and R.M. revised the manuscript. All authors have read and agreed to the published version of the manuscript.

FUNDING

This research was partly funded by the Portuguese Foundation for Science and Technology (FCT), through projects MEDWATERICE (PRIMA/0006/2018), supported by national funds (PIDDAC), projects UIDB/04292/2020 and UIDP/04292/2020 granted to MARE – Marine and Environmental Research Center, University of Coimbra (Portugal), strategic project UIDB/04450/2020 granted to RISCO – Research Centre for Risks and Sustainability in Construction, and project LA/P/0069/2020 granted to the Associate Laboratory ARNET – Aquatic Research Network, supported by national funds. The author S.Z. was granted a PhD fellowship from FCT (Ref. 2020.07183.BD).

ACKNOWLEDGEMENTS

The authors express their gratitude to Bruno Matos, Jean Tavares at the Instituto Federal de Educação, Ciência e Tecnologia do Rio Grande do Norte (IFRN) and Rui Pedroso de Lima at the Innovative Dynamic Monitoring for Water Quality and Ecology (INDYMO) for their help in conducting the fieldwork. Additionally, the authors would like to acknowledge Hydrology Research, the Euromediterranean Network of Experimental and Representative Basins (ERB) – 18th Biennial Conference 2022 and Daniele Penna, the current coordinator of the ERB, for the sponsorship in publishing this research.

DATA AVAILABILITY STATEMENT

All relevant data are included in the paper or its Supplementary Information.

CONFLICT OF INTEREST

The authors declare there is no conflict.

REFERENCES

Abrantes, J. R., Moruzzi, R. B., Silveira, A. & de Lima, J. L. M. P. 2018 Comparison of thermal, salt and dye tracing to estimate shallow flow velocities: novel triple-tracer approach. *Journal of Hydrology* **557**, 362–377. https://doi.org/10.1016/j.jhydrol.2017.12.048.

Abrantes, J. R., Moruzzi, R. B., de Lima, J. L. M. P., Silveira, A. & Montenegro, A. A. 2019 Combining a thermal tracer with a transport model to estimate shallow flow velocities. *Physics and Chemistry of the Earth, Parts A/B/C* **109**, 59–69. https://doi.org/10.1016/j.pce.2018.12.005.

Aley, T. & Fletcher, M. W. 1976 The water tracer's cookbook. *Missouri Speleology* **16** (3), 1–32. https://doi.org/10.1016/S0341-8162(02)00149-2.

Buzády, A., Erostyák, J. & Paál, G. 2006 Determination of uranine tracer dye from underground water of Mecsek Hill, Hungary. *Journal of Biochemical and Biophysical Methods* **69** (1–2), 207–214. https://doi.org/10.1002/9780470747148.

de Lima, J. L. M. P. & Abrantes, J. R. C. B. 2014 Using a thermal tracer to estimate overland and rill flow velocities. *Earth Surface Processes and Landforms* **30** (10), 1293–1300. https://doi.org/10.1002/esp.3523.

de Lima, R. L., Abrantes, J. R., de Lima, J. L. M. P. & de Lima, M. I. P. 2015 Using thermal tracers to estimate flow velocities of shallow flows: laboratory and field experiments. *Journal of Hydrology and Hydromechanics* **63** (3), 255–262. https://doi.org/10.1515/johh-2015-0028.

de Lima, J. L. M. P., Zehsaz, S., de Lima, M. I. P., Isidoro, J. M., Jorge, R. G. & Martins, R. G. 2021 Using quinine as a fluorescent tracer to estimate overland flow velocities on bare soil: proof of concept under controlled laboratory conditions. *Agronomy* **11** (7), 1444. https://doi.org/10.3390/agronomy11071444.

de Lima, J. L. M. P., Zehsaz, S., Tavares, J. L. & de Lima, M. I. P. 2023 Brightness of point application of fluorescent quinine tracer for surface waters. *Engenharia Sanitária E Ambiental*. **28**, e20220212.

Diener, H. C., Dethlefsen, U., Dethlefsen-Gruber, S. & Verbeek, P. 2002 Effectiveness of quinine in treating muscle cramps: a double-blind, placebo-controlled, parallel-group, multicentre trial. *International Journal of Clinical Practice* **56** (4), 243–246.

EFSA Panel on Food Contact Materials, Enzymes, Flavourings and Processing Aids (CEF) 2015 Scientific opinion on flavouring group evaluation 35, revision 1 (FGE. 35rev1): three quinine salts from the priority list from chemical group 30. *EFSA Journal* **13** (9), 4245. https://doi.org/10.2903/j.efsa.2015.4245.

Fulton, J. W., Anderson, I. E., Chiu, C. L., Sommer, W., Adams, J. D., Moramarco, T., Bjerklie, D. M., Fulford, J. M., Sloan, J. L., Best, H. R. & Conaway, J. S. 2020 QCam: SUAS-based doppler radar for measuring river discharge. *Remote Sensing* **12** (20), 3317. https://doi.org/10.3390/rs12203317.

Geto, A., Amare, M., Tessema, M. & Admassie, S. 2012 Polymer-modified glassy carbon electrode for the electrochemical detection of quinine in human urine and pharmaceutical formulations. *Analytical and Bioanalytical Chemistry* **404** (2), 525–530. https://doi.org/10.1007/s00216-012-6171-8.

Gilley, J. E., Finkner, S. C., Doran, J. W. & Kottwitz, E. R. 1990 Adsorption of bromide tracers onto sediment. *Applied Engineering in Agriculture* **6** (1), 35–38. https://doi.org/10.13031/2013.26341.

Lei, T., Chuo, R., Zhao, J., Shi, X. & Liu, L. 2010 An improved method for shallow water flow velocity measurement with practical electrolyte inputs. *Journal of Hydrology* **390** (1–2), 45–56. https://doi.org/10.1016/j.jhydrol.2010.06.029.

Leibundgut, C., Maloszewski, P. & Külls, C. 2009 *Tracers in Hydrology*. Wiley-Blackwell, John Wiley & Sons Ltd. https://doi.org/10.1002/9780470747148.

Manfreda, S., McCabe, M. F., Miller, P. E., Lucas, R., Pajuelo Madrigal, V., Mallinis, G., Ben Dor, E., Helman, D., Estes, L., Ciraolo, G. & Müllerová, J. 2018 On the use of unmanned aerial systems for environmental monitoring. *Remote Sensing* **10** (4), 641. https://doi.org/10.3390/rs10040641.

Masafu, C., Williams, R., Shi, X., Yuan, Q. & Trigg, M. 2022 Unpiloted Aerial Vehicle (UAV) image velocimetry for validation of two-dimensional hydraulic model simulations. *Journal of Hydrology* **612**, 128217. https://doi.org/10.1016/j.jhydrol.2022.128217.

Moorthy, J. N., Shevchenko, T., Magon, A. & Bohne, C. 1998 Paper acidity estimation: application of pH-dependent fluorescence probes. *Journal of Photochemistry and Photobiology A: Chemistry* **113** (2), 189–195. https://doi.org/10.1016/S1010-6030(97)00332-8.

Mujtaba, B. & de Lima, J. L. 2018 Laboratory testing of a new thermal tracer for infrared-based PTV technique for shallow overland flows. *Catena* **169**, 69–79. https://doi.org/10.1016/j.catena.2018.05.030.

Schuetz, T., Weiler, M., Lange, J. & Stoelzle, M. 2012 Two-dimensional assessment of solute transport in shallow waters with thermal imaging and heated water. *Advances in Water Resources* **43**, 67–75. https://doi.org/10.1016/j.advwatres.2012.03.013.

Su, T. C. 2017 A study of a matching pixel by pixel (MPP) algorithm to establish an empirical model of water quality mapping, as based on unmanned aerial vehicle (UAV) images. *International Journal of Applied Earth Observation and Geoinformation* **58**, 213–224. https://doi.org/10.1016/j.jag.2017.02.011.

Tauro, F., Grimaldi, S., Petroselli, A., Rulli, M. C. & Porfiri, M. 2012 Fluorescent particle tracers in surface hydrology: a proof of concept in a semi-natural hillslope. *Hydrology and Earth System Sciences* **16** (8), 2973. https://doi.org/10.5194/hess-16-2973-2012.

Tauro, F., Pagano, C., Phamduy, P., Grimaldi, S. & Porfiri, M. 2015 Large-scale particle image velocimetry from an unmanned aerial vehicle. *IEEE/ASME Transactions on Mechatronics* **20** (6), 3269–3275. https://doi.org/10.1109/tmech.2015.2408112.

Thermo Fisher Scientific. 2021 *Safety Data Sheet Quinine Monohydrochloride Dihydrate 99%*. Available from: https://www.alfa.com/en/msds/?language=EN&subformat=AGHS&sku=H33474 (accessed on 14 March 2022).

Tmušić, G., Manfreda, S., Aasen, H., James, M. R., Gonçalves, G., Ben-Dor, E., Brook, A., Polinova, M., Arranz, J. J., Mészáros, J. & Zhuang, R. 2020 Current practices in UAS-based environmental monitoring. *Remote Sensing* **12** (6), 1001. https://doi.org/10.3390/rs12061001.

Zehsaz, S., de Lima, J. L., de Lima, M. I. P., Isidoro, J. M. & Martins, R. 2022 Estimating sheet flow velocities using quinine as a fluorescent tracer: bare, mulched, vegetated and paved surfaces. *Agronomy* **12** (11), 2687. https://doi.org/10.3390/agronomy12112687.

Zhang, G. H., Luo, R. T., Cao, Y., Shen, R. C. & Zhang, X. C. 2010 Correction factor to dye-measured flow velocity under varying water and sediment discharges. *Journal of Hydrology* **389** (1–2), 205–213. https://doi.org/10.1016/j.jhydrol.2010.05.050.

First received 27 January 2023; accepted in revised form 2 May 2023. Available online 19 May 2023